

10wt.% NaOH Alloy 600 SCC

The Effect of Heat Treatment and Stress on SCC Behavior of Alloy 600 in 10wt.% NaOH Solution

150

220

Alloy 600 의 응력부식파괴(stress corrosion cracking, SCC) 거동을 315℃의 10wt.% NaOH 수용액에서 C-ring 을 이용하여 평가하였다. SCC 시험은 부식전위보다 200mV 높은 전위에서 수행하였다. 시편을 다양하게 열처리하여 입계의 예민화 정도와 입계탄화물의 밀도를 변화시켰다. C-ring 의 apex 에 가해진 응력은 상온 항복응력의 각각 150%와 250%가 되도록 하였다. 가해진 응력이 250%일때 열처리에 관계없이 10 일 이내에 균열이 발생하였고, 150%의 경우 HTMA 를 제외하고는 균열이 발생하지 않았다. 315℃의 10wt.% NaOH 수용액에서 SCC 저항성은 HTMA, HTMA+SEN, HTMA+TT 순서로 증가하였으며, 응력이 증가할수록 SCC 속도는 증가하였다. 균열이 발생한 시편을 10 도 간격으로 구분하여 관찰한 결과 HTMA+TT 가장 균일한 균열분포를 보였고, AES 분석을 통해 C-ring 의 외부표면과 균열부위의 최외각 표면에서 Cr 이 고갈되고, Ni 이 농축됨을 관찰했다.

ABSTRACT

Stress corrosion cracking (SCC) of Alloy 600 has been studied in 10wt.% NaOH at 315 . SCC test was performed using C-ring specimen at the potential of +200mV above corrosion potential in 10wt.% NaOH solution. The tubing materials were systematically heat treated to control degree of sensitization and intergranular carbide distribution. Stress at the apex of C-ring specimen was in the range from 150 to 250% of room temperature yield strength. SCC of Alloy 600 was found in 10days for stress of 250% yield strength at the apex of C-ring but was not found in 10days for stress of 150% except for HTMA. The SCC resistance of Alloy 600 increased with a following sequence: HTMA, HTMA+SEN and HTMA+TT. SCC rate increased with stress at the apex of C-ring. The cracked C-ring specimen were sectioned by the 10 degree interval, and it was observed that HTMA+TT had most uniform crack distribution . The outermost surface films of both outer

surface and SCC fracture surface were enriched in Ni and depleted in Cr by Auger Electron spectroscopy analysis.

1.

1960, Alloy 600 SCC Alloy

600 Alloy 600 Alloy 600, Copson¹⁻³⁾ 1 2

Alloy 600, Coriou^{4,5)}

(stress corrosion cracking, SCC)가 Alloy 600 SCC 가

Alloy 600 SCC 가 Alloy 600 SCC 가 Pb가

Alloy 600 SCC 가 Alloy 600 SCC 가 SCC

가 (open circuit potential, OCP) 100 - 300mV SCC가

6,7,15) 가 SCC

sleeving plugging 2

(pH)가 가 가 2

가 SCC Na

가¹⁶⁾ SCC 2

, molar ratio 가

17) SCC

가 SCC

Alloy 600 SCC

가 가

2.

Alloy 600 as received Alloy 600 high temperature mill annealed (HTMA) Alloy 600, HTMA Alloy 600

가 600 24 (SEN), 715 15

(HTMA+SEN) TT (HTMA+TT)

Alloy 600 98M θ + (2M θ) 5

etching SEM

315 10% NaOH, reference electrode external Ag/AgCl

C-ring, ASTM G.38 bolt loading

가 , C-ring apex 150 250%가
 polarization curve
 +200mV vs. E_{corr} 가 EG&G 273A potentiostat
 SEM
 apex 10
 SCC
 deposit Auger depth profile

3.

가. HTMA 600 Table 1, 2
 Fig.1 . SEN 600 Cr 가
 가 HTMA 600 가 , line coverage TT 600 . TT 600
 가 가

Table 1 chemical composition of HTMA 600

Designation	Ni	Cr	Fe	C	S	P	B	N	Si	Cu	Al	Ti
HT 600	75.14	15.46	8.42	0.025	0.001	0.008	0.0039	0.0042	0.16	0.011	0.21	0.29

Table 2. Cr concentration at grain boundary, intergranular carbide thickness, width and line coverage and SCC rate

Alloy	Cr depletion	Intergranular carbide			Max. CGR ($\times 10^{-10}$ m/sec)
	Min. Cr conc. (wt.%)	Length(μ m)	Thickness(μ m)	Line coverage(%)	250% of
HT 600	13.2	0.28	0.15	28	10.45
SN 600	7.3	0.41	0.20	89	9.96
TT 600	10.5	0.57	0.29	80	9.47

SCC test

Alloy 600 315°C Fig.2 가 315°C
 300mV가 , 가 315°C 10³

Fig. 3 C-ring +200mV 10 가
 가 , apex . Table

3 150 250% 가
 가 , HTMA SCC 가
 , TT 가 가 , Cr

(,) 10% NaOH . Fig. 4

. Fig. 5 C-ring apex 10

. Fig. 6

7 , Fig. 7 TT 600 가 가 가 , Fig. 6 가

Table 3. Maximum SCC rate($\times 10^{-10}$ m/sec) in 10wt % NaOH at 315 .

Stress(% of yield strength)	HTMA	HTMA+SEN	HTMA+TT
150	0.35<	No crack	No crack
250	10.45	9.96	9.47

. AES
Fig. 8 9 HTMA, TT

(A)
depth profile . Fig. 10 normalizig HTMA, SEN, TT
, SCC ,
. HTMA , 가
4.7 μ m , TT 10 μ m . TT
HTMA
. Normalizing , , 3
Ni enrichment Cr depletion .

4.

10 10wt.% NaOH C-ring apex 250% Alloy 600
SCC HTMA, HTMA+SEN, HTMA+TT 가 , 150%
가 HTMA 0.358 $\times 10^{-10}$ m/sec , HTMA+SEN
HTMA+TT 가 SCC 가 .
HTMA+SEN 가 가 HTMA SCC 가 ,
HTMA+SEN HTMA
C-ring 10 TT
가 가 .
AES 10wt.% NaOH deposit layer Cr
, Ni가 , .
가 .

1. H. R. Copson and W. E. Berry, Corrosion, Vol. 16, No. 2, p. 79t, 1960.
2. H. R. Copson and W. E. Berry, Corrosion, Vol. 18, No. 1, p. 21t, 1962.
3. H. R. Copson and S. W. Dean, Corrosion, Vol. 21, No. 1, p. 1, 1965.
4. H. Coriou, L. Grall, Y. LeGall and S. Vettier, Stress corrosion cracking of Inconel in high temperature water, Saclay, North Holland Pub. Co., Amsterdam, The Netherlands. p. 161, 1959.
5. H. Coriou, L. Grall, C. Mathieu and M. Pelas, Corrosion, Vol. 22, No. 10, p.280, 1966.
6. N. Pessall, G. P. Airey and B. P. Lingenfelter, Corrosion, Vol. 35, No. 2, p. 100, 1979.
7. R. Bandy, R. Roberge and D. van Rooyen, EPRI NP-4458,p. A10-1, 1986.
8. Ph. Berge, J. R. Donati, B. Prieux, and D. Villard, Corrosion, Vol.33, p. 425, 1977.
9. G. J. Theus, Corrosion, Vol. 33, p. 2, 1977.
10. J. F. Newman, EPRI NP-3043, 1983.
11. W. H. Cullen, M. J. Partridge and F. Hernandez-Arroyo, Proceedings of Sixth International Symposium on Environmental Degradation of Materials in Nuclear Power Systems - Water Reactors, p.197, 1993.
12. E. Pierson, J. Stubbe, W. H. Cullen, S.M. Kazanjian and P. N. Paine, Proceedings of Seventh International Symposium on Environmental Degradation of Materials in Nuclear Power Systems - Water Reactors p. 303, 1995.
13. M. Helie, Sixth International Symposium on Environmental Degradation of Materials in Nuclear Power Systems - Water Reactors, p. 179, 1993.
14. S. S. Hwang, K. M. Kim and U. C. Kim, Eighth International Symposium on Environmental Degradation of Materials in Nuclear Power Systems - Water Reactors, p. 200, 1997.
15. S. Suzuki. T. Kusakabe,H. Yamamoto, K. Aorika and T.Ochi, Fifth International Symposium on Environmental Degradation of Materials in Nuclear Power Systems - Water Reactors, p. 861, 1991.
16. R. J. Jacko, EPRI NP-6721-SD, 1990.
17. J. A. Gorman and A. P. L. Turner, Proceedings of meeting, Improving the Understanding and Control of Corrosion on the Secondary Side of Steam Generators, Airlie, VA, October 9-13,1995 ,NACE, Houston, p. 85, 1996.

Figures.

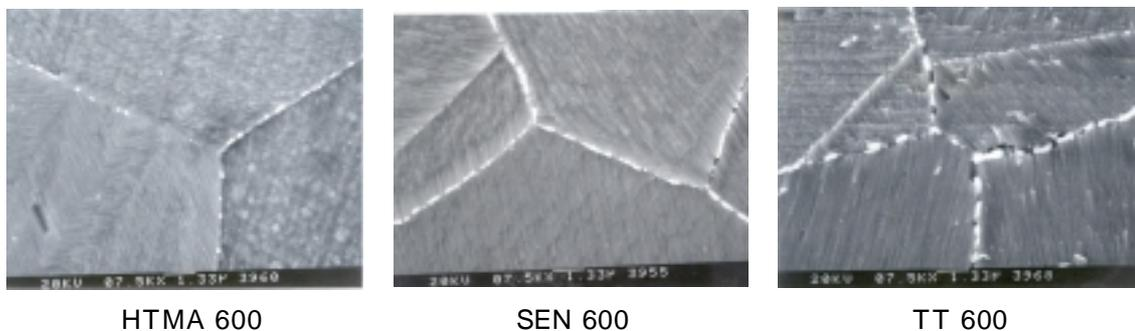


Fig. 1. Intergranular carbide distribution in Alloy 600 observed after etching in bromine solution.

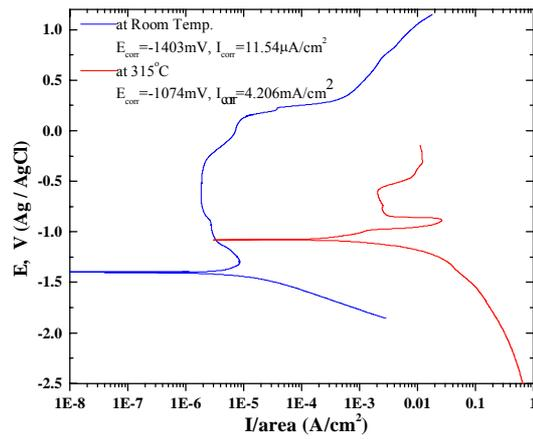


Fig. 2. Polarization curve of Alloy 600 in 10wt% NaOH solution at room temperature and 315°C.

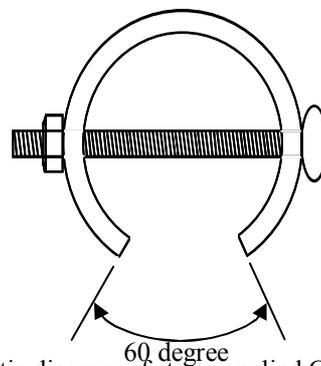


Fig. 3 . Schematic diagram of stress applied C-ring specimen.

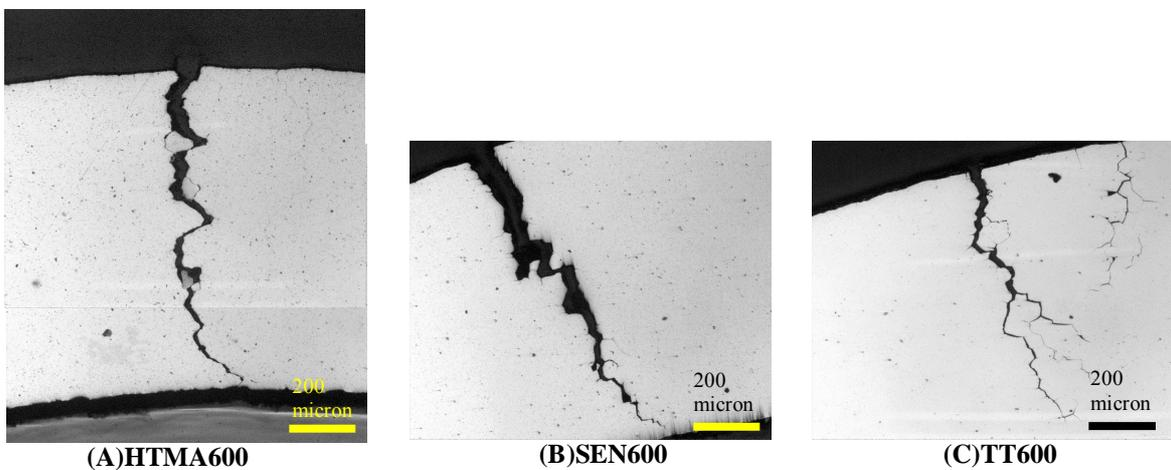


Fig. 4. Cross sectional area of (A)HTMA 600, (B)SEN 600 (C)TT 600 showing maximum SCC length exposed to 10wt.% NaOH at 315 for 10days.

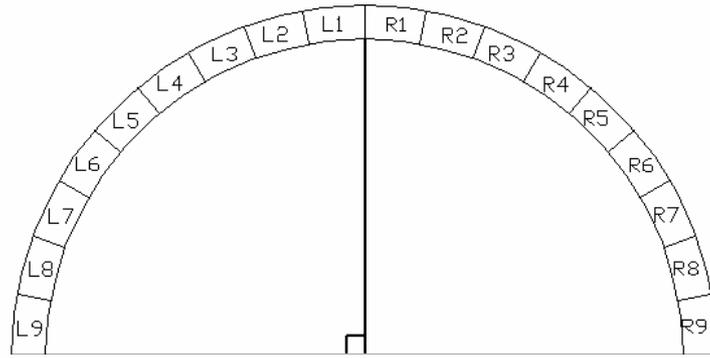


Fig. 5 Schematic diagram of sectional district of C-ring specimen by the 10 degree.

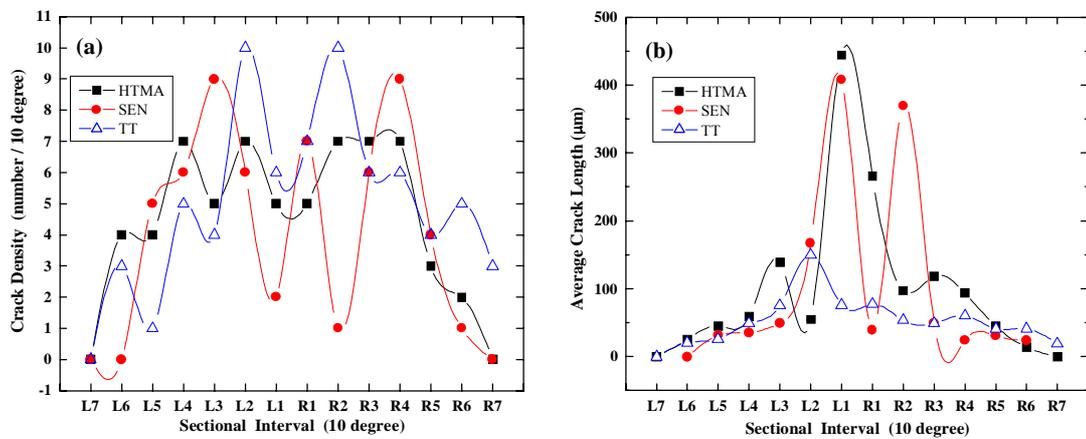


Fig. 6 Crack density(a) and average crack length(b) distribution in sectional district of C-ring specimen by the 10 degree interval.

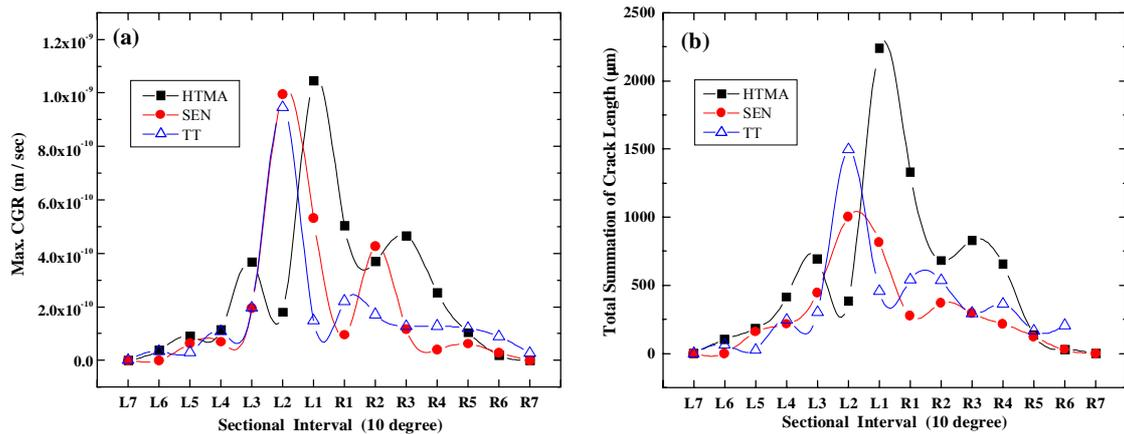


Fig. 7 Distribution of Max. CGR(a) and total crack length summation(b) in sectional district of C-ring specimen by the 10 degree interval.

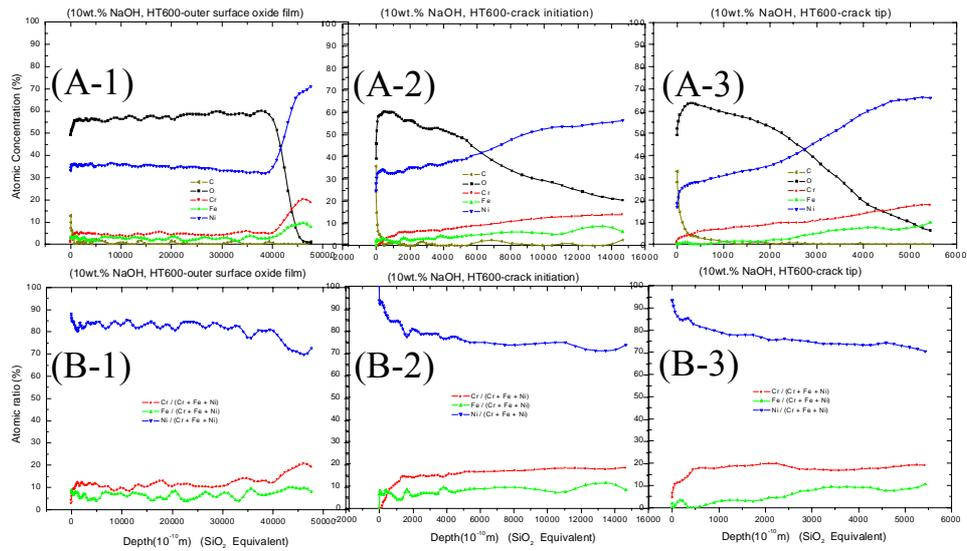


Fig. 8. AES depth profiles at passive film of the HT 600 after applied potential to 0.2Vocp exposed to 10wt.% NaOH for 10days: (A)before and (B)after normalization

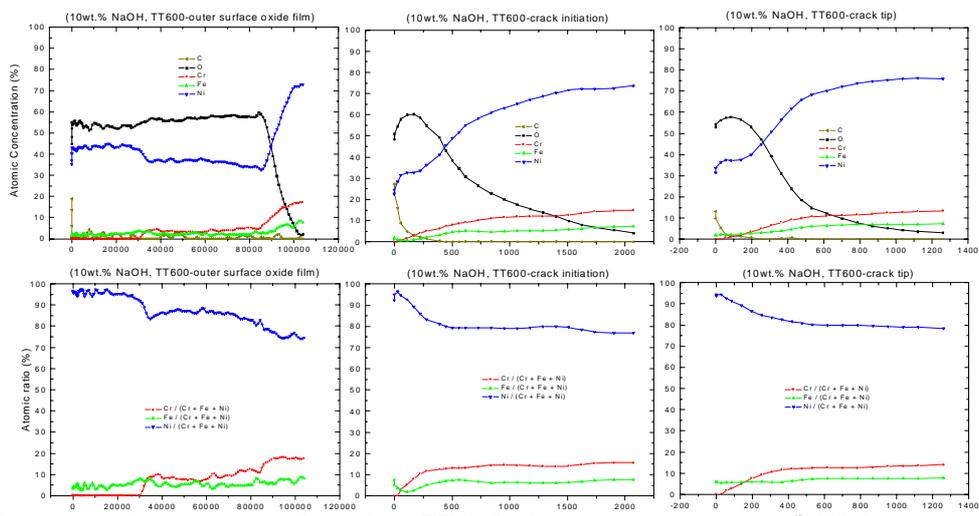


Fig. 9 AES depth profiles at passive film of the TT 600 after applied potential to 0.2Vocp exposed to 10wt.% NaOH for 10days: (A)before and (B)after normalization

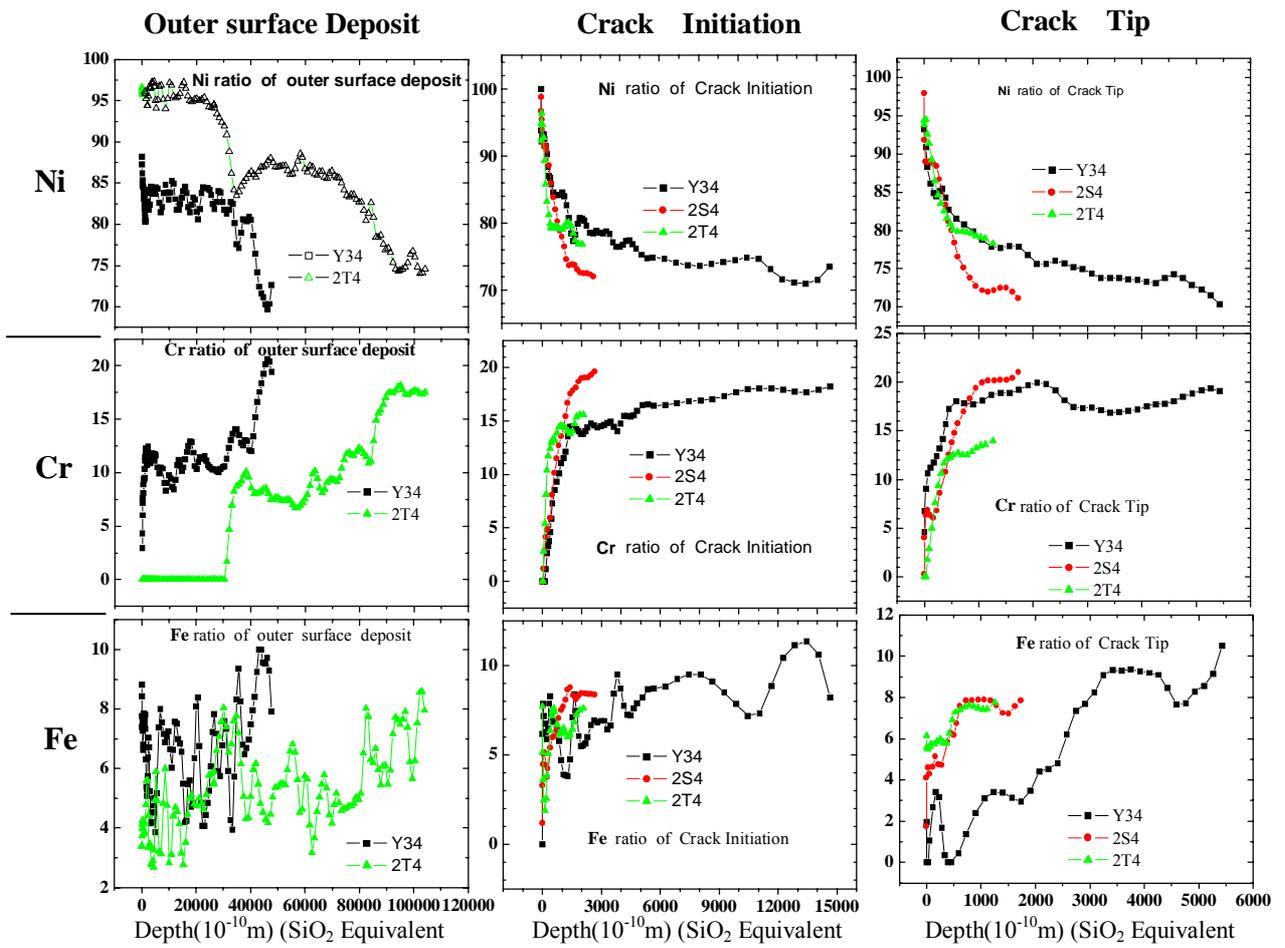


Fig. 10 AES depth profiles at passive film of the HT600, TT 600 and SEN600 after applied potential to 0.2Vocp exposed to 10wt.% NaOH for 10days ; plots are after normalization.